ViF-GTAD: A new Automotive Dataset with Ground Truth for ADAS/AD Development, Testing and Validation

Journal Title
XX(X):1–14

DOI: 10.1177/ToBeAssigned
www.sagepub.com/
SAGE

Sarah Haas[1], Selim Solmaz[1], Jakob Reckenzaun[1], Simon Genser[1]

Abstract

A new dataset for automated driving, which is the subject matter of this paper, identifies and addresses a gap in existing similar perception datasets. While most state-of-the-art perception datasets primarily focus on the provision of various onboard sensor measurements along with the semantic information under various driving conditions, the provided information is often insufficient since the object list and position data provided include unknown and time-varying errors. The current paper and the associated dataset describe the first publicly available perception measurement data that include not only the on-board sensor information from the camera, Lidar, and radar with semantically classified objects but also the high precision ground-truth position measurements enabled by the accurate RTK-assisted GPS localization systems available on both the ego vehicle and the dynamic target objects. This paper provides insight on the capturing of the data, explicitly explaining the metadata structure and the content, as well as the potential application examples where it has been, and can potentially be, applied and implemented in relation to automated driving and environmental perception systems development, testing, and validation.

Keywords

Automotive Dataset; ADAS; Ground Truth; GPS; Sensor Models; Sensor Fusion; Localization

1 Introduction

Considering the fact that the majority of traffic accidents are induced by human errors, road traffic safety can be significantly increased by utilizing advanced driver assistance systems (ADAS) and automated driving (AD). There are several studies indicating this fact e.g., as shown by Lundgren and Tapani (2006) in simulation and Hannawald and Kühn (2015) by traffic data analysis. These ADAS/AD functions, in connection with several other measures, are part of the European Commission (2019) "Road Safety Policy Framework" and are expected to play a crucial role in the EU's 'vision-zero' goal. In addition, ADAS/AD functions are expected to deliver additional benefits. Fagnant and Kockelman (2015) predict benefits like higher transport efficiency, better mobility accessibility for elderly people, increased convenience and comfort, and new business models like car sharing in the long term.

Despite the broad variety of safety and mobility benefits, the mass market uptake of ADAS/AD functions and especially the release of vehicles with higher autonomy levels (i.e. SAE level 3+ vehicles, where the autonomy levels are defined by the SAE J3016) are rather slow compared to initial predictions. A recent study Doll et al. (2020) predicts that Level 2+ systems are going to be the main growth drivers in the automated driving market. ISO PAS 1883:2020 defines that systems labeled as SAE Level-3 with 'conditional driving automation', can handle dynamic driving tasks (DDT) under certain conditions known as the operational design domain (ODD). The driver can take the eyes off the road and is only required to react to a take-over request to control the vehicle.

The shift from Level-2 to Level-3 is a huge leap as the responsibility of environment perception and safety assurance is transferred from the driver in Level-2 to the automated driving system (ADS) in Level-3 vehicles. This requires a reliable environment perception system (EPS). EPS usually utilizes a combination of several sensors, possibly including multiple cameras, radars, lidars as well as ultrasonic sensors with superfluous combinations. EPS is also tasked with the processing and contextual fusion of the massive amounts of corresponding sensor data. To the authors' best knowledge, there are only two officially approved and road-legal SAE Level-3 systems available on the market, namely the Mercedes Drive Pilot Daimler (2021) and Honda Sensing Elite system Honda (2020), both of which provide L3 automation under certain ODDs.

"Honda Sensing Elite" is a suite of advanced safety and driver-assistive (ADAS) technologies currently available on Honda vehicles. The Honda Legend Hybrid EX Sedan is the first vehicle to be offered to end customers with the world's first certified Level 3 autonomous driving technology, starting in March 2021.The Mercedes Drive Pilot is another conditionally automated Level-3 self-driving technology capable of monitoring the environment and performing all tasks without driver intervention until it actively requests the driver to take the wheel. In the new 2021 S-Class, the

[1]Virtual Vehicle Research GmbH, Graz, Austria

Corresponding author:
Dr. Selim Solmaz, Virtual Vehicle Research GmbH, Control Systems Group, Inffeldgasse 21a, 8010 Graz, AT.
Email: selim.solmaz@v2c2.at

Drive Pilot takes over these tasks. However, it only works up to a speed of 60 km/h, which is the autonomous driving speed currently permitted in Germany. The limitation of maximum velocity is also in line with the restrictions of the first version within the UNECE R157 Regulation 157 on the "Approval of Automated Lane Keeping Systems (ALKS)", the first and probably most comprehensive international policy issued for the approval of ADS. These two examples show that, although released to the market, the mass-market accessibility, availability, and respective uptake of highly automated vehicles, let alone the SAE Level-3 vehicles with conditional automation, is still very low.

The rules and regulations for automotive vehicle type approval are under constant development and improvement. UNECE R157 with its two amendments is just one example focusing on the ALKS, for the changes in many approval-relevant documents. Another example is the release of a draft "New process-oriented" automated driving type approval approach (for SAE Level-3+ vehicles) described in the document UNECE WP.29.

While the current state-of-the-art in automation and robotics can potentially allow higher levels of autonomy in ADS, lack of proper testing, verification, and validation procedures hinder the development and mass-market utilization of such systems Solmaz et al. (2021b,a). The classical automotive testing and validation approaches for certifying automated vehicles would require several millions of kilometers of on-road testing time and are practically unfeasible Kalra and Paddock (2016). Simulation techniques can potentially be utilized for this purpose, but the fidelity and modeling accuracy requirements need to be further investigated as pointed out by Dueser et al. (2019).

Towards virtual testing of automated driving systems, recently completed SetLevel Project proposed four sensor model fidelity levels in the order of increasing fidelity as reported in Rainer Aue (2022):

1. Idealized Sensor model,
2. Stochastic Sensor model,
3. Phenomenological Sensor model,
4. Physical Sensor model.

Each fidelity level model can provide various individual features, which may suit different modeling needs, particularly in the context of EPS. To drive the development and testing of highly automated systems further, more diverse and novel testing approaches as well as utilization of more accurate datasets with additional information are required.

Datasets are typically utilized during the development phase of the EPS for AI-based algorithm development, verification, and validation steps. Such datasets usually contain recorded sensor data along with semantic information in the form of labeled objects. This information is typically utilized for object detection and classification development and testing pipelines. Additionally, these datasets can also be used for the development of specific features for specific sensor model types. However, precise position information of the external objects is missing in such datasets.

We present in this paper a new dataset that we name ViF-GTAD after "**Vi**rtuelles **F**ahrzeug - **G**round **T**ruth dataset for **A**utomated **D**riving". The fact that all traffic objects within the driving scenarios have ground-truth position information, as ascertained by the extremely precise RTK-GPS systems employed in each car, distinguishes this dataset from others in the literature. In doing so, the corresponding position information of each vehicle was calibrated precisely before the measurement runs, and the mounting positions of the GPS antennas as well as the dimensions of the vehicles were taken into account.

The current paper describes the new ViF-GTAD dataset Haas et al. (2023), which should serve as a user manual for the associated data recordings of a set of typical driving scenarios. The dataset contains 5 different scenarios that are representative of typical test cases for ADAS function approval as well as requirements for sensor model development. The development of sensor model features is also reflected in the scenario selection. In the paper, we also discuss other possible application areas for the corresponding dataset with examples that could aid ADAS and ADS development.

The remainder of this paper is organized as follows. In Section 2, we analyze state of the art in automotive datasets and provide a comparison between them in terms of information content. In Section 3, we first introduce the measurement campaign enabling the collection of the corresponding data in subsection 3.1 as well as the vehicle configuration and setup in subsection 3.2. Then we describe the data content and structure in detail for each sensor data in subsection 3.3 and then define the test scenarios in subsection 3.4. In Section 4 we describe 3 specific use cases where the described data can potentially be utilized in relation to EPS development. Finally, the conclusions and future work are given in Section 5. A list of commonly used nomenclature is also given at the end of the text.

2 Related Work

In this section, an overview of the currently available public datasets with comparable content to the ViF-GTAD dataset is given. Most of these datasets are commonly utilized for automated driving and perception algorithm development, verification, and validation purposes in the literature.

The A2D2 dataset Geyer et al. (2020) was recorded in 3 German cities and provides semantic segmentation images, semantic point clouds, and annotations 3D bounding box for a smaller part of the dataset.

The ApolloScape Huang et al. (2020) project provides different datasets including, e.g., annotated Lidar point cloud and stereo camera datasets for object detection, manually annotated trajectories for prediction algorithms, and several more. The data was recorded in a large city in China with heavy traffic.

ArgoVerse offers 2 datasets (Chang et al. (2019), Wilson et al. (2021)) where both have been recorded in cities in the USA. Both datasets contain HD maps and partly annotated Lidar and stereo camera scenarios. The second also contains trajectory information for targets and generally refines and extends the first dataset.

The BDD100K dataset Yu et al. (2020) provides labeled 3D bounding box data and semantic segmentation data based on cameras recorded in several different US cities and rural areas under different weather and time of day conditions.

Table 1. List of currently available datasets for autonomous driving. The list shows the sensor data included in the corresponding dataset.

Dataset	Lidar	Radar	Camera	GPS Ego	GPS Targets	Additional Information
A2D2 Geyer et al. (2020)	✓		✓			3D bounding boxes
ApolloScape Huang et al. (2020)	✓		✓	✓		
Argoverse1 Chang et al. (2019)	✓		✓	✓		3D bounding boxes
Argoverse2 Wilson et al. (2021)	✓		✓	✓		3D bounding boxes
BDD100K UC Berkeley Yu et al. (2020)			✓	✓		Lane markings, 3D bounding boxes
Brno Urban Ligocki et al. (2020)	✓	✓	✓	✓		YOLO-classified camera images
CADCD Pitropov et al. (2020)	✓		✓	✓		Adverse weather, 3D bounding boxes
CityScapes Cordts et al. (2016)			✓	✓		Semantic information
Dense Bijelic et al. (2020)	✓	✓	✓			Road friction sensor, weather station data, 3D bounding boxes
EU Long-term Dataset Yan et al. (2020)	✓	✓	✓	✓		
Ford AV Agarwal et al. (2020)	✓		✓	✓		
Honda 3D Patil et al. (2019)	✓			✓		3D bounding boxes
Kitti Geiger et al. (2013)	✓		✓	✓		
Leddar PixSet Déziel et al. (2021)	✓	✓	✓	✓		One Solid-state and one mechanical lidar
Woven Perception Houston et al. (2020)	✓		✓			3D bounding boxes
Málaga Urban Blanco-Claraco et al. (2014)	✓		✓	✓		
NuScenes Caesar et al. (2020)	✓	✓	✓	✓		3D bounding boxes
Oxford RoboCar Maddern et al. (2017)	✓		✓	✓		
PandaSet Scale (2021)	✓		✓	✓		
Radiate Sheeny et al. (2020)	✓	✓	✓	✓		
Waymo Perception Ettinger et al. (2021)	✓		✓			3D bounding boxes
ViF-GTAD Haas et al. (2023)	✓	✓	(✓)	✓	✓	Lane markings and objects from MobilEye instead of raw images

The Brno Urban dataset Ligocki et al. (2020) provides YOLO-classified camera images with 2D bounding boxes. The dataset was taken in urban, suburban, and highway areas around Brno, Czech Republic, in varying weather and lighting conditions.

CADCD Pitropov et al. (2020) focuses on the effects of adverse weather on automotive Lidar and cameras including labeled 3D bounding boxes. It was recorded in the city and rural areas in the Waterloo region in Canada during winter.

The CityScapes dataset Cordts et al. (2016) focuses on semantic segmentation of urban street scenarios and was recorded in around 50 German cities. The dataset features dense semantic segmentation and instance segmentation for 30 classes of objects.

Dense Bijelic et al. (2020) features a variety of datasets focused on the effects of various weather conditions on a large amount of different automotive sensors. The dataset partly includes annotated 3D bounding boxes and covers thousands of kilometers in urban and rural areas around northern Europe.

The EU long-term dataset Yan et al. (2020) utilizes 11 sensors with highly overlapping fields of view. It was recorded mostly in downtown and some sub-urban areas in Montbéliard, France, in varying daytime and weather conditions. It includes a large number of roundabouts.

Ford AV Agarwal et al. (2020) provides data recorded in different weather, lighting, and traffic conditions all around Michigan, USA, including the city of Detroit that was collected over the course of more than 1 year. It also provides 3D mapping data for the driven routes.

The 3D dataset by Honda Patil et al. (2019) includes annotated 3D bounding boxes with 8 classes of objects in crowded and traffic intense areas around several US cities. It aims to provide data for 3D object detection and tracking algorithms.

The Kitti dataset Geiger et al. (2013) provides data for 3D object detection and tracking as well as pixel and instance-level semantic data. The dataset was recorded in urban, rural, and highway areas around Karlsruhe, Germany.

The PixSet by Leddar Déziel et al. (2021) includes annotated 3D bounding box data with 22 classes of objects. It provides full-waveform data from a solid-state Lidar and was recorded in high-density urban and suburban areas around Canada in different weather conditions.

The Woven perception dataset Houston et al. (2020) (previously Lyft) offers annotated 3D bounding boxes for raw camera and Lidar data and HD semantic maps collected in urban and suburban areas around Palo Alto, USA, to support the development of object detection algorithms.

The Malaga urban dataset Blanco-Claraco et al. (2014) offers high-resolution and high-rate data from stereo cameras and Lidar in various urban scenarios around Malaga to provide data for computer vision algorithms in automotive applications.

NuScenes Caesar et al. (2020) offers an annotated 3D bounding box for parts of the various scenarios collected with 13 automotive sensors in 2 traffic-dense cities. The

sensors cover a 360° view around the vehicle to provide data for perception algorithms in autonomous driving.

The Oxford RoboCar dataset Maddern et al. (2017) offers around 100 runs of the same route over the course of more than one year in various weather, lighting and traffic conditions taken in Oxford, UK, to allow for long-term experiments on localization and mapping of dynamic urban environments.

PandaSet Scale (2021) provides labeled 3D bounding boxes with 28 object annotation classes as well as segmented point clouds with 37 segmentation labels. The dataset was recorded in urban areas around San Francisco, USA.

The Radiate dataset Sheeny et al. (2020) provides data for several sensors, e.g., high-resolution 2D annotated radar data, collected in urban and highway scenarios around Edinburgh, UK. It focuses on various adverse weather conditions as well as different lighting conditions.

Waymo Open Perception Ettinger et al. (2021) offers labeled 2D and 3D bounding boxes as well as HD maps and labeled 2D and 3D semantic data in various urban scenarios recorded around San Francisco, USA.

Table 1 lists the above-named datasets in a more comprehensive way highlighting the sensor configuration and dataset-specific additional information for each dataset. The last row indicates the corresponding information for the new ViF-GTAD dataset. As can be observed from Table 1, high-precision GPS positions (i.e., the ground truth information) of the target objects are available only in the new ViF-GTAD dataset.

While most of the datasets utilize similar sensor configurations and provide bounding boxes, some popular examples such as the Kitti Geiger et al. (2013), the CityScapes Cordts et al. (2016), and the NuScenes Caesar et al. (2020) do not contain the accuracy information regarding object-list provided.

In Section 4 possible applications of this dataset are shown, especially under focus are use cases where the ground-truth information about all targets is a major benefit or even required. For example, the proposed sensor model training approach in Section 4.1 is based on the comparison of tracked object data from a sensor and the ground-truth position of the tracked vehicle. This means only with the introduced dataset, the training of this sensor model is possible. For other applications such as sensor fusion, or lidar localization, see Sections 4.2 and 4.3, the ground-truth information of all targets enables testing and validation of the developed approaches.

3 The ViF-GTAD Dataset

Ground truth refers to the true, real-world state of the environment in the context of automotive vehicles, such as the position, speed, and direction of other vehicles, pedestrians, and obstacles, as well as road conditions such as the location of lanes, traffic signals, and stop signs. Ground truth is typically classified as static and dynamic. The static ground truth, as the name implies, includes all static objects in the environment. (e.g. road layout, traffic signs, buildings, road infrastructure, etc.). In contrast, dynamic ground truth represents all moving objects relative to the static world (e.g., VRUs, vehicles, etc.) around the ego-vehicle.

In this section, we describe the ViF-GTAD dataset in detail including the test campaign, vehicle setup, data structure, and test scenarios involved. The ViF-GTAD dataset is available to download from the following public repository: Haas et al. (2023).

First, we describe the data acquisition campaign explaining the capturing of the static ground truth and the dynamic ground truth of the target vehicles. Later in the section, we explain the ego-vehicle measurement setup and then the structure and content of the new dataset with the ground truth information.

3.1 TestEPS Measurement Campaign

The data collection was made in the scope of a recent exploratory project named TestEPS aiming at a transnational testing region development for automated driving and environmental perception systems. The exploratory projects TestEPS and CentralSystem prepared two larger projects within the EUREKA cluster (details of the project can be found in Reckenzaun et al. (2022)). While the data collection was done in the exploratory phase, the data preparation for public release was done within the EUREKA project. More details about the measurement campaign and data are available on request from BME (2020). The exploratory project is the result of a bilateral agreement on the ministerial level between Hungary and Austria in 2017 for fostering cooperation on the testing and development of connected, automated vehicles. Several partners joined the measurement campaign resulting in a test vehicle fleet of 13 vehicles including passenger vehicles of various sizes along with a truck and a semi-trailer.

The actual measurement was conducted on a closed measurement section (GNSS coordinates: 47.625778, 17.270162) near the Hungarian city of Csorna in the last week of June 2020. Csorna is a small town in North-West Hungary, close to the crossing of two main regional highway sections, M85 and M86.

The measurement was done on Section-1 (red) and Section-2 (blue) of the motorway stretch as illustrated in Figure 1. Section-1 serves as an interchange area where the two carriageways (M85 & M86) have different horizontal and vertical alignments. The road sections in each direction have two 3.50-m-wide lanes for the through traffic, and there are also additional accelerating/decelerating lanes linked to junction ramps. In contrast, Section-2 can be categorized as an open highway with a roughly 300-m-long dual carriageway section including two 3.50-m-wide traffic lanes, and 3.00 m wide hard shoulder on both sides, in each direction.

Static ground truth is usually captured using vehicles equipped with highly sophisticated measurement equipment. Measurement of the static ground truth is easier compared to the dynamic counterpart since several measurement runs can be conducted on the measurement section and the individual measurement runs can be combined. Such a repetitive process enables the detection of blind spots and smooths the individual faulty measurement points.

Dynamic ground truth, on the other hand, can be obtained by fusing information from a multitude of sources including road infrastructure sensors, drones, as well as onboard sensors on the test vehicles. For the dataset generation as part

Figure 1. Sections of the test site (3.5 km in all) located near Csorna city (Hungary) on route E65

of this test campaign, the only common requirement for the measurement vehicles was to include a high-precision GNSS system with RTK corrections which were used to capture the dynamic ground truth of the target vehicles. All the test vehicles in this scope had different sensor configurations other than the high-precision GNSS localization systems, which were individually calibrated to measure the exact antenna mounting positions and the vehicle outer dimensions for the calculation of accurate bounding boxes.

Further details on the measurement campaign can be found in an initial publication on the measurement campaign Tihanyi et al. (2021).

3.2 Vehicle setup and measurement hardware

As an active player in ADAS/AD system development, Virtual Vehicle Research GmbH also took part in the measurement campaign, as described in the preceding section, with one of its generic Automated Drive Demonstrator (ADD) vehicles. The Ford Fusion Hybrid MY2017 (seen in Figure 2) was the vehicle used for this purpose, which is equipped with several additional sensors and computational hardware as well as custom software components.

Figure 2. ViF's Automated Drive Demonstrator (ADD) Vehicle.

First and foremost, the ADD vehicle is equipped with the DataSpeed drive-by-Wire Kit*, which enables access to most of CAN data as well as the control actuators for ADAS/AD system development. The ADD Vehicle is also equipped with additional sensors, which can be modified depending on the measurement or the use-case requirements. To support the aims of the measurement campaign, the ADD vehicle was equipped with a high-accuracy dual-antenna DGPS system to provide ground truth position information. A Novatel ProPak6 RTK-GPS receiver was utilized for the measurement of the precise position supported by TCP/IP-based RTK correction service providing sustained cm-level accuracy. Additionally, the ADD vehicle also logged other sensor data relevant to the perception algorithm development and validation purposes. These sensors specifically included a MobilEye630 intelligent camera, a Continental ARS408 Radar† and an Ouster OS1-64 Lidar sensor‡. Figure 3 shows the mounting positions of these perception sensors. For the data acquisition, ROS-based Autoware.AI§ software stack running on an Ubuntu X86-PC was utilized to log the data in rosbag format. In table 2, detailed measurement values for the position of the sensors in the vehicle are to be used for the transformation of each sensor's data into a common coordinate system. The origin of the coordinate system for all transformations is the center of the rear axle on the vehicle. All transformation values are, of course, also included in the data files provided in the dataset. The GPS module's position is not given in the table as it is located directly at the origin at the center of the rear axle and has no offset.

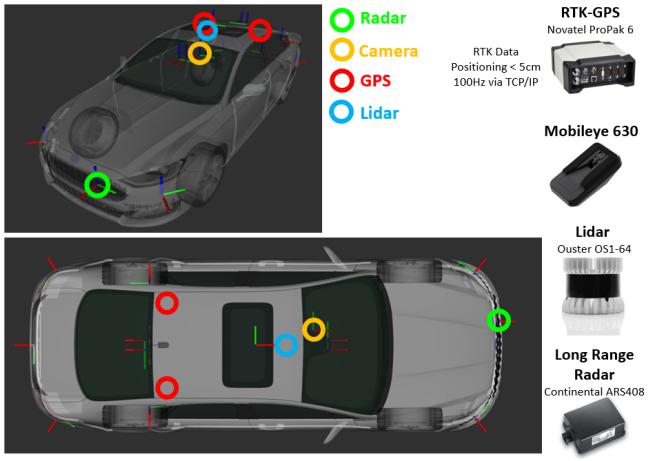

Figure 3. ViF's ADD-Vehicle sensor setup and the corresponding mounting positions.

Table 2. The positional offsets of the sensors with respect to the middle of the rear axle in meter. The x-axis is pointing along the driving direction, the y-axis to the left, and the z-axis towards the sky.

Sensor	Offset in x, y, z [m]
Ouster OS-1 Lidar	1.625, 0.0, 1.19
Continental ARS408 Radar	3.75, 0.25, 0.5
Mobileye630 Camera	1.85, 0.15, 0.95

*https://www.dataspeedinc.com/
†https://conti-engineering.com/components/ars-408/
‡https://ouster.com/products/os1-lidar-sensor/
§https://www.autoware.ai/

3.3 Dataset Structure

Internally, ROS uses so-called nodes to, e.g., receive and preprocess data from a sensor, execute algorithms using specific data, or command actuators to execute actions. These nodes send messages to each other using a publish-subscribe principle. The nodes publish data to certain topics and subscribe to other topics to receive data from other nodes. The data logging mechanism is rather simple as the user can either log every message sent between the ROS nodes or can explicitly state the nodes whose messages should be stored. Each stored entry in the rosbag file consists of a Unix format timestamp, the topic as a string, and the message itself. The messages themselves vary widely in their structure as they can contain any kind of data format, data type, and structure defined by the node that generated the message. In our case, the Ford Fusion stored the messages of a total of 39 different topics with 23 different data types for the messages (see Figure 4 for an excerpt of topics in the rosbags). We will not give the structural details of each of these topics as this would exceed the scope of this paper but focus on the messages from the Ouster OS1-64 Lidar sensor, the MobilEye630 series intelligent camera, the Continental ARS408 Radar, and the Novatel ProPak6 RTK-GPS receiver. Furthermore, we will give the structure of the GPS data of the other vehicles in the measurement campaign.

```
rosbag
├─ /camera0/camera_info
├─ /can_bus_1/can_rx
├─ /gps/corr_imu
├─ /gps/enhanced_fix
├─ ...
├─ /mobileye/objects
├─ /mobileye/roadmarkings_list
├─ /tracked_objects_mobileye
├─ /os1_cloud_node/points
├─ /os1_img_node/intensity_image
├─ ...
├─ /sensor/lrr_front/clusters
├─ /sensor/lrr_front/clusters_specific
└─ /tf
```

Figure 4. Excerpt of topics included in a rosbag file recorded by our test vehicle.

3.3.1 Ouster OS1-64 Lidar Data Structure: The Ouster OS1-64 Lidar generates a point cloud with 64 layers where each layer provides up to 2048 points. The raw data for each point consists, amongst other parameters, of the measured range, angle, and reflectivity. From these parameters, several topics are generated in our test vehicle to allow for easier usage and post-processing of the raw data. Table 3 shows the published topics related to the Ouster OS1-64 on our test vehicle. For example, the topic *os1_cloud_node/points* contains messages of the ROS data type *PointCloud2*[¶] to represent the 3D point cloud of one recorded frame.

Each $PointCloud2$ consists of the information of a point cloud frame with several data parameters including data, width, height, fields, etc. The $data$ field contains the information for each single point of the point cloud. The structure of the Ouster OS1-64 Lidar data can be seen in Table 4.

Table 3. Most important topics with the corresponding data type of the Ouster OS1-64 Lidar on our test vehicle.

Topic	Data type
/os1_cloud_node/imu	sensor_msgs/Imu
/os1_cloud_node/points	sensor_msgs/PointCloud2
/os1_img_node/intensity_image	sensor_msgs/Image
/os1_img_node/noise_image	sensor_msgs/Image
/os1_img_node/range_image	sensor_msgs/Image

3.3.2 MobilEye630 Camera Data Structure: The MobilEye630 camera is equipped with object detection software that allows identification and tracking of other vehicles, pedestrians, bicycles, etc., detection of road markings and traffic signs, and the taking of black-and-white images. The raw data cannot be accessed as the camera directly computes the 3D bounding boxes for the detected objects, an estimation of the distance and headings of the objects, and the information and location of lane markings and traffic signs. Table 5 shows the most important published topics on our test vehicle related to the MobilEye630 camera.

For each frame, the MobilEye630 camera produces a list of objects, lane markings, and traffic signs. In Table 6, Table 7, and Table 8, the most important parameters regarding the object data, road markings data, and traffic sign data produced by the camera can be seen.

3.3.3 Continental ARS408 Radar Data Structure: The Continental ARS408 Radar is a long-range Radar with up to 250 m detection range. It generates a list of cluster points for detected objects. A single object can generate several cluster points depending on its size, reflectivity, and angle with respect to the radar's position. The topics recorded on our test vehicle can be seen in Table 9.

The `clusters` topic is a post-processed list extracted from the `clusters_specific` list and contains a list of the calculated Cartesian coordinates for the lateral and longitudinal offset of each cluster point as well as velocity, standard deviation, and the radar cross-section value. Table 10 shows the most important parameters related to the clusters.

3.3.4 Novatel ProPak6 RTK-GPS Data Structure: The Novatel ProPak6 is a high-precision GPS module installed in the middle of the rear axis on our test vehicle. It uses RTK support to further enhance the precision of the vehicle's position compared to plain GPS. It produces a large number of topics that can be seen in Table 11.

The most important topic is `/gps/ins_pvax` since it includes the GPS time data, the position, orientation, and standard deviation of position and orientation. The most important parameters related to this topic can be seen in Table 12.

[¶] https://docs.ros.org/en/melodic/api/sensor_msgs/html/msg/PointCloud2.html

Table 4. Parameters with the corresponding data types of the Ouster OS1-64 Lidar on our test vehicle.

Parameter	Description	Unit	Value Range
x, y, z	Cartesian coordinates	m	$\pm$ Range of Lidar (Float)
intensity	number of photons reflected from surface	-	Int
reflectivity	calculated from intensity using a characteristic curve	-	Int
ring	Detecting layer on sensor	-	0 - (#rings - 1) (Int)
range	Distance to hit surface	mm	0 - Range of Lidar (Double)
t	Time until laser response received	ns	64-bit Int

Table 5. Most important topics with the corresponding data type of the MobilEye630 Camera on our test vehicle.

Topic	Data type
/mobileye/objects	common_msgs/ObjectList
/mobileye/roadmarkings_list	environment_model_msg/RoadMarkings
/mobileye/trafficsigns_list	environment_model_msg/TrafficSignList

Table 6. Most important parameters with the corresponding data types of the MobilEye630's object list on our test vehicle.

Parameter	Description	Unit	Value Range
id	Unique Id of the object	-	Int
existence_probability	General probability of the object's existence	-	Float
class_probability	Probability of object classes (e.g. car, truck, etc.)	%	0-1 (Float)
position	x/y/z coordinates of the bounding box center	m	0 - Range (Float)
orientation	quaternions of the bounding box	-	Float
dimension	width/length/height of bounding box	m	Float
acceleration	directional accelerations of the bounding box	$\frac{m}{s^2}$	Float
co-variance	Standard deviations for each physical quantity	-	Float

Table 7. Most important parameters with the corresponding data types of road markings detected by the MobilEye630 on our test vehicle.

Parameter	Description	Unit	Value Range
quality	Enum of the quality of lane measurement	-	Int
width	Width of detected lane	m	[0 - 2.5]
coefficients	Parameters of the cubic polynomial of detected lane	-	Float
lane_type	Enum type of detected lane	-	Int
type	left or right lane	-	Int

Table 8. Parameters with the corresponding data types of the traffic signs detected by the MobilEye630 on our test vehicle.

Parameter	Description	Unit	Value Range
id	Unique Id of the object	-	Int
valid	Correct detection of the sign	-	0 or 1
sign_type	Enum for different signs	-	Int
supplement_type	Enum for supplementary signs	-	Int
position	x/y/z coordinates of the center of the traffic sign	m	0 - Range (Float)

Table 9. Most important topics with the corresponding data type of the Continental ARS408 Radar on our test vehicle.

Topic	Data type
/sensor/lrr_front/clusters	common_msgs/ClusterList
/sensor/lrr_front/clusters_specific	continental_msgs/ClusterListARS408

Table 10. Most important parameters with the corresponding data types of the Continental ARS408 clusters on our test vehicle.

Parameter	Description	Unit	Value Range
position	x/y/z coordinates of the cluster point	m	Float
velocity	velocity in x/y/z directions	$\frac{m}{s}$	Float
position_std_dev	Standard deviation of the position	-	Float
velocity_std_dev	Standard deviation of the position	-	Float
rcs	radar cross-section	-	Float

3.3.5 GPS Data Structure of Target Vehicles: All other vehicles included in the dataset created GPS tracks as well. The structure of the GPS tracks for each vehicle is identical and can be seen in Table 13. Additionally, the positions of the GPS devices on the vehicle are provided. The data structure can be seen in Table 14.

Table 11. Most important topics with the corresponding data type of the Novatel ProPak6 RTK-GPS on our test vehicle.

Topic	Data type
/gps/corr_imu	novatel_gps_eth_msgs/CorrImu
/gps/enhanced_fix	gps_common/GPSFix
/gps/fix	sensor_msgs/NavSatFix
/gps/gga	std_msgs/String
/gps/imz	sensor_msgs/Imu
/gps/ins_pvax	novatel_gps_eth_msgs/InsPvax
/gps/ins_status	std_msgs/String
/gps/pos_type	std_msgs/String
/gps/utm_odom	nav_msgs/Odometry

3.3.6 GPS calibration process: All the vehicles taking part in the measurement campaign were equipped with RTK-supported GNSS for high-precision localization. All the GNSS systems were calibrated for accurate positioning results before being utilized in the actual measurement runs on the M86 high-way road stretch. This calibration process was conducted on the ZalaZONE ‖ proving ground.

At the first step of the calibration process, the same TCP/IP-based RTK correction service (NTRIP**) on each test vehicle was set up. On the next step, a specific reference point was selected on the ZalaZONE proving ground and a ground marking was drawn. In order to determine the GNSS measurement uncertainties, the test vehicles were positioned exactly at this reference point. For each vehicle, the front number plate and the ground marking were aligned and the onboard GNSS system position information was recorded. Then, utilizing the mounting position of the antennas as well as the outer dimensions of the vehicle, the accuracy information was obtained and calibration in relation to the reference point was completed.

3.4 Test Scenarios

In this subsection, we introduce 5 scenarios included in the dataset. It needs to be pointed out that the tests were conducted exclusively with manually driven vehicles since the focus was gathering ground truth data. The measurements were done during daylight and under good weather conditions (sunny with some scattered clouds).

The selection of the 5 scenarios is mainly motivated by the existing testing standards for ADAS function approval tests as well as requirements for sensor model development. For example, for the ACC ISO 20035:2019 (E) and ALKS UNECE R157 approval tests, Test-Scenario-1, Test-Scenario-2, and Test-Scenario-4 are relevant use cases for evaluation. Scenarios 2-5 on the other hand, are useful for sensor model development and validation purposes, where an example of the probabilistic camera model development for the MobilEye630 camera utilizing this dataset was reported recently by the authors in Genser et al. (2021), with a summary given as an application use case later in Section 4.1.

Test-Scenario-1 (Cut-in): In this scenario, 5 vehicles were moving at a constant speed (with approximately 10-20 km/h) as depicted in Figure 5 on two lanes. The ego vehicle was driving in the left lane before cutting in suddenly to the free space in front of the last vehicle.

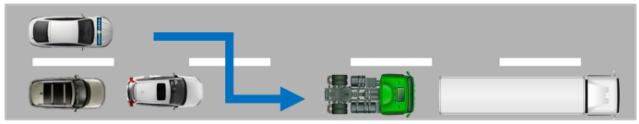

Figure 5. Test scenario-1 with ego vehicle cutting-in.

Test-Scenario-2 (Occlusion): In this scenario, a convoy of 5 vehicles was moving at a constant speed (with approximately 10-20 km/h) according to Figure 6, while distances between the vehicles were varied equally. The ego vehicle was in the furthermost position behind the convoy. The target distances between each vehicle were set consecutively as 1m, 5m, 10m, 30m, and 50m.

Figure 6. Test scenario-2 with ego vehicle at the rear.

Test-Scenario-3 (Separability): In this scenario, 3 vehicles were standing next to each other as depicted in Figure 7 with the ego vehicle placed behind in the middle lane. The 3 target vehicles drove slowly away (around 10-20km/h) while the ego vehicle stayed stationary or vice-versa.

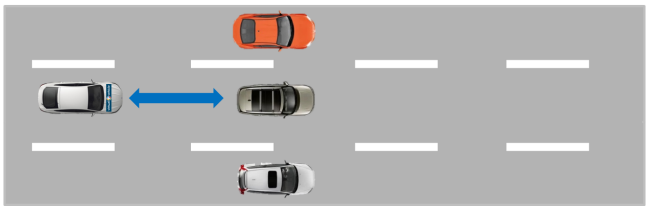

Figure 7. Test scenario-3 with three targets increasing distance to ego vehicle.

Test-Scenario-4 (Overtake by a truck): In scenario 4, depicted in Figure 8, the ego vehicle first overtakes a truck-trailer. After this maneuver, the vehicle decelerates and reduces speed. Then the truck-trailer approaches and overtakes the ego vehicle on the right. Finally, the ego vehicle accelerates and overtakes the trailer again.

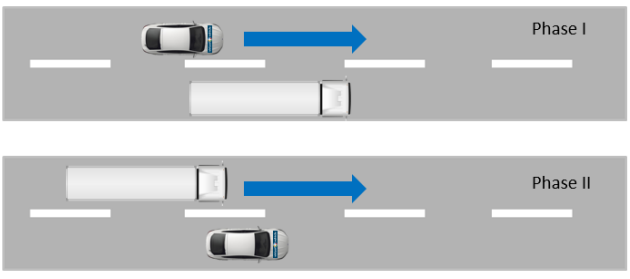

Figure 8. Test scenario-4 Overtaking of Truck

‖ https://zalazone.hu/

** https://igs.bkg.bund.de/ntrip/about

Table 12. Most important parameters with the corresponding data types of the Novatel GPS data on our test vehicle.

Parameter	Description	Unit	Value Range
latitude	latitude of the GPS position	°	Float
longitude	longitude latitude of the GPS position	°	Float
height	Elevation above sea level	m	Float
roll_deg	roll angle of the vehicle	°	Float
pitch_deg	pitch angle of the vehicle	°	Float
azimuth_deg	azimuth angle or heading of the vehicle	°	Float
std	Standard deviations of all physical quantities	-	Float
week_number	week number in GPS calendar	-	Int
week_seconds	seconds since week started	-	Float

Table 13. Parameters with the corresponding data type of the GPS data structure of the other vehicles involved in the measurement campaign.

Parameter	Description	Unit	Value Range
Time	date and time (format: '25-06-2020 11:01:11.790')	-	String
Latitude	latitude of the GPS position	°	Float
Longitude	longitude latitude of the GPS position	°	Float
LatStdDev	latitude standard deviation	-	Float
LongStdDev	longitude standard deviation	-	Float
Heading	Heading of the vehicle	°	Float

Table 14. Parameters of the GPS vehicle position on the vehicles involved in the measurement campaign.

Parameter	Description	Unit
Participant	Name of the participant	-
Car Type	Type and name of the used vehicle	-
Offset From Front	position offset from front license plate along the vehicle length	cm
Offset From Middle	position offset from the middle along the vehicle's width	cm

Test-Scenario-5 (Stationary and flowing traffic): Scenario 5, depicted in Figure 9, has three phases. In the initial phase, the ego vehicle comes to a still stand just in front of the single trailer. In the second phase, the single truck is overtaken on the right by a convoy of vehicles including a passenger vehicle, a truck with a trailer attached, and a Smart. After this maneuver is done, the ego vehicle accelerates and overtakes the convoy in the second lane. Starting from the initial situation again, Phase I and Phase II are repeated.

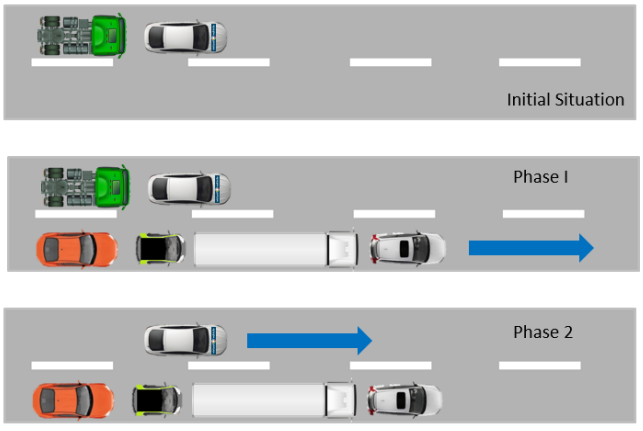

Figure 9. Test scenario-5 Stationary and flowing traffic

4 Application Use Cases

In order to demonstrate the utility of the new automotive dataset with ground truth information, we give in this section various application use cases or examples, which either utilize the dataset (Section 4.1) or are direct observations from it (Sections 4.2 and 4.3) calling for deeper analysis and further exploitation. Even though these application examples are relevant to general automotive systems development, they are particularly useful for perception systems development for automated driving.

4.1 Sensor Model Development

In this first use case, we present how the ViF-GTAD dataset with ground-truth information can be utilized for sensor model development. We shall do so by describing a sensor model of the MobileEye camera utilizing the MobileEye camera data (i.e., dynamic object lists) and the dynamic ground-truth data (i.e., the positions of other traffic objects). A possible approach for this, which is explained in detail in a recent paper by the authors Genser et al. (2021), will be summarized below.

The basic idea is to model detection errors of the MobilEye camera, as they are known as a result of the availability of the dynamic ground-truth data of every traffic object involved in the test scenarios (see Section 3.4). Every perception sensor, also including the MobileEye camera, consists of a field of view (FoV), which is a circular segment defined by an angle and a range. In the first step of modeling, every object outside the FoV or occluded by other objects is removed from the input object list. Every remaining entry in the object list is given to the core of the model, where the so-called kernel density estimation theory is combined with the classical linear regression theory for the modeling of the distance-based detection error and the natural scattering

of the camera. In Figure 10 and Figure 11 a representative comparison of this camera model against the ground-truth data and the actual MobilEye measurement data are shown. In both figures it can be seen that the simulated sensor model is closer to the measured data comparing it to the ground-truth, therefore the use of this sensor model is generating more realistic sensor data than just taking the ground-truth information. For a more detailed analysis see Genser et al. (2021).

As a test case, one object from the previously described scenarios has been utilized, which was omitted in the training data for this sensor model, as this would falsify the results. Here the results indicate that the sensor model fits well with the measured data, and especially the scattering of the camera is modeled satisfactorily.

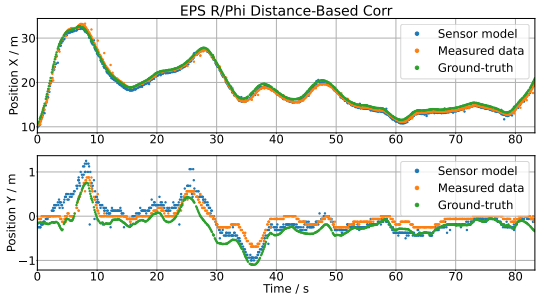

Figure 10. Results of developed MobileEye camera model utilizing the ViF-GTAD dataset with ground-truth data.

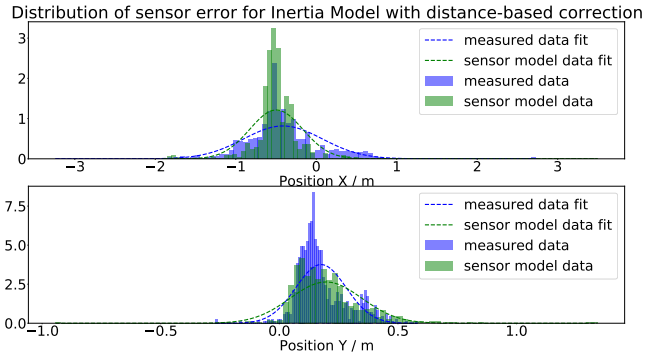

Figure 11. Comparisons of the Gaussian fit of the divergence of the measured (MobilEye630) and simulated sensor data from the ground-truth utilizing the ViF-GTAD dataset.

4.2 Development and Testing of Sensor Fusion Algorithms

The second use case example of how the ViF-GTAD dataset can be used in the scope of automated driving concerns the development and testing of sensor fusion algorithms. Multi-sensor fusion is a commonly utilized technique in automated driving to improve the robustness of the corresponding perception algorithms. This originates from the fact that each environmental sensor has a number of weaknesses (e.g., poor low-light performance of cameras, interference, cross-talk in radar, etc.), which can be alleviated by using redundant sensor modalities to combine the benefits of each sensor. This ensures that corresponding perception algorithms work with higher performance and confidence under changing environmental conditions, which in turn increases the availability of the corresponding ADAS/AD functions.

ViF-GTAD dataset contains three main environmental sensor modalities including lidar, radar, and camera, which are typically used in automated driving vehicles in superfluous combinations. These sensors can be combined in different ways to enable testing and validation of newly developed sensor fusion algorithms thanks to the GPS ground-truth data available from the target objects. The GPS-based ground-truth tracks of each target vehicle should allow testing of the perception and sensor fusion algorithms against the measured values. This should particularly be useful for example, for testing multi-object tracking and object detection algorithms.

The radar sensor can measure the speed of a target object, detect occluded objects, is only very slightly influenced by adverse weather, and has no issues with changing illumination conditions. It is, however, very hard to detect the exact location, size or shape of an object with a radar. An object can reflect n radar points depending on the material properties and the shape of the object. These reflections can be in any position on the object, making it hard to determine the exact location and size of an object.

Lidar on the other hand can detect the exact position, shape, and size of an object thanks to a dense point cloud generated, and has only very minor issues with bad lighting conditions. Lidar, however, cannot detect the speed of an object efficiently, cannot see past an obstacle, and has issues with bad weather conditions.

The MobilEye camera can be used to detect and classify objects in a scene very easily. It has issues, however, with longitudinal position (distance) and size estimation of an object, and cannot see past obstacles. Furthermore, it has low performance in adverse weather as well as low-light conditions due to reduced visibility, and also cannot efficiently cope with rapidly changing illumination.

In Figure 12 a birdseye-view of one frame in scenario 3 can be seen. The green bounding boxes are generated from the GPS coordinates of the corresponding vehicles and transformed into the ego coordinate system to allow for a comparison of the bounding box with the lidar and radar points. Figure 13 the same frame can be seen from an ego perspective. Here the shapes of the vehicles detected by the lidar can be seen clearly. In both images, it can be seen, that the bounding boxes match the points of lidar and radar quite well. Since there is always a standard deviation for measured data from sensors, the bounding boxes and sensor measurements do not correlate perfectly. The standard deviations for each GPS measurement are given in the files. The data sheets of the sensors give standard deviations as well which makes it possible to incorporate these parameters in any calculation. Autonomous driving functions in real life need to deal with such standard deviations since the sensor data they rely on, always come with a standard deviation. Therefore, by considering such effects already in the design phase of AD functions, the reliability of the function can be increased.

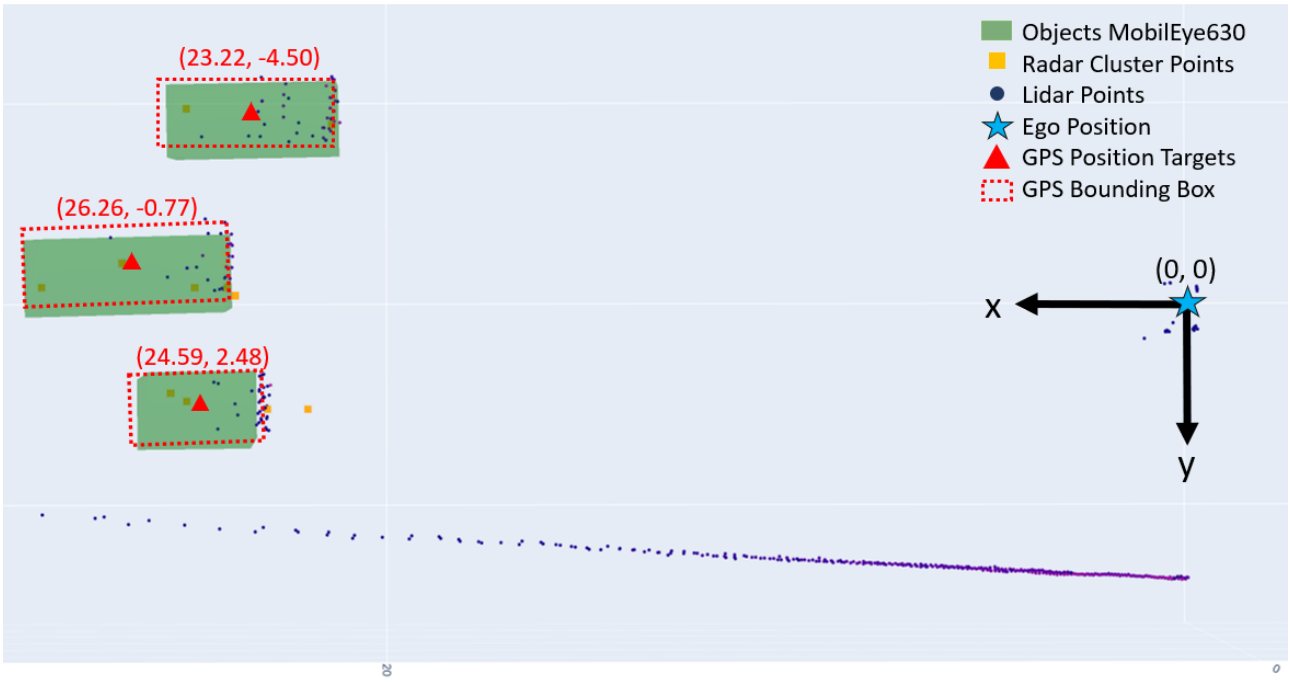

Figure 12. Birdseye-view of one frame of scenario 3. The ego vehicle is positioned at the origin of the coordinate systems. The tuples in brackets above each bounding box are referring to the GPS position (red triangle) of the vehicle in meters with respect to the ego vehicle.

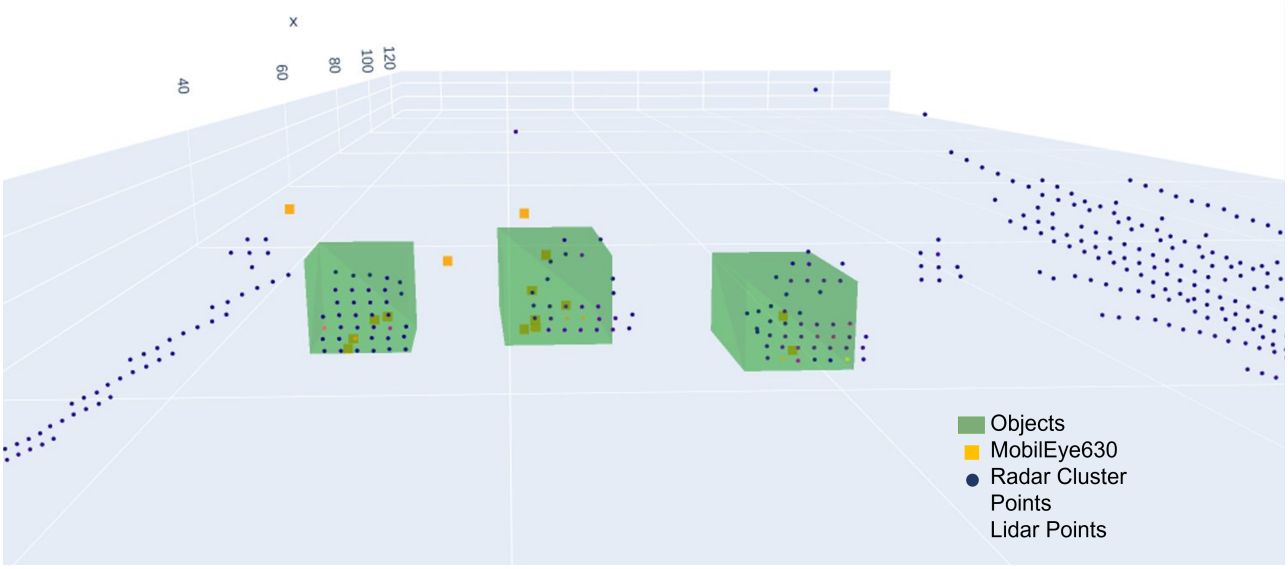

Figure 13. View of the same frame as in Figure 12 from the ego's perspective.

Now, we give specific examples of how different sets of these sensors can be combined or fused with possible benefits and potential deficiencies.

4.2.1 Lidar+Radar Fusion: Lidar and radar in combination would allow for the detection of a non-occluded object with its speed and shape. This would allow, e.g., a classification of the object or a prediction of its behavior. In this case, occluded objects can still be detected but with uncertainty in their shape and exact position.

4.2.2 Radar+Camera Fusion: A combination of radar and camera would allow for the detection of speed, distance, and class of each object in the field of view of both sensors. While occluded objects can still be recognized, their exact location, shape, and class can not be determined with certainty.

4.2.3 Lidar+Camera Fusion: A combination of lidar and camera would allow for an exact determination of the position, shape and class of an object. However, occluded objects remain hidden and the speed of objects cannot be determined easily.

4.2.4 Radar+Lidar+Camera Fusion: A combination of the three sensors would allow for the detection of speed, distance, position, shape, and class of each non-occluded object in the field of view of all three sensors. Occluded objects can still be recognized, though their exact location, shape, and class can not be determined with certainty.

The analysis of the ViF-GTAD dataset resulted in interesting observations, for example regarding the radar reflections from a truck-trailer combination. Radar-only reflections may be quite insufficient in clustering and classifying them as a truck or a set of closely driving cars, whereas a combination with lidar or camera may easily solve this issue.

4.3 Lidar-based Localization

In the third use case example for the ViF-GTAD dataset, we look at the localization problem utilizing lidar sensors and describe how the dataset can be used as the basis for evaluating the performance of such localization algorithms.

Localization of the ego vehicle as well as the other objects around the vehicle is a crucial part of autonomous driving. Ego vehicle localization is typically achieved with GNSS data, or utilizing a 3D map in conjunction with lidar based on an algorithm such as the NDT (normal distributions transform) matching. Based on ego localization, relative localization of the surrounding objects can be made. Lidar point clouds can be used to determine the shape, size, and position of an object. This makes lidar an ideal choice for localization purposes. To localize the surrounding objects, the ego vehicle can either communicate with the other objects to inquire about their positions or measure their positions themselves utilizing the onboard environmental sensors. Since communication with other objects is not always possible since, e.g., pedestrians won't send their position to the ego vehicle, a precise localization pipeline of surrounding objects is essential for accurate and continuous assessment of the environment as a basis for the decision-making process. Accurate and high-precision estimation of the position of the surrounding objects allows for safe and efficient navigation and enables better reactions in emergency situations.

The ViF-GTAD dataset provides lidar point clouds, the highly-accurate GPS tracks of target vehicles, the exact location of the GPS modules on the target vehicles, and the precise dimensions of each target vehicle. Therefore, a lidar-based localization pipeline for external object detection could easily be tested and verified using this dataset.

Accurate bounding boxes as well as the exact shapes of the target vehicles can be generated, and placed at the measured precise GPS positions. The lidar point clouds generated by our test vehicle as part of the ViF-GTAD dataset can be used as input to object detection as well as the localization pipelines and the results can be compared with the GNSS-based target vehicle bounding boxes to determine the accuracy of the localization/object-detection pipelines. In doing so, the position and orientation of the GNSS-based (ground-truth) target vehicle bounding boxes with that of the lidar point-cloud-based ones at different distances, angles, and speeds should be a good basis for comparison to measure the respective spatial and temporal performances of the perception pipelines. Such a study is planned as a future work for this paper.

5 Conclusion

This paper provided insight into the capturing of the ViF GTAD dataset, explicitly explaining the content and metadata structure.

A drawback of current state-of-the-art public datasets is that they only provide ground truth data from the perspective of the ego vehicle. In addition to the captured in-vehicle sensor data, this dataset also provides GNSS ground truth data of the target vehicles.

Another issue of many public datasets is limited or missing provisioning of metadata. Within this paper, we give precise and highly accurate descriptions of the metadata, strictly following the FAIR data usage principle to enable easy and simple reuse of the provided data.

By showing three use cases building on the ViF-GTAD dataset, an idea of the potential that rests in the usage of the dataset was shown. This work is of high relevance as it can be, applied and implemented in relation to automated driving and environmental perception systems development, testing, and validation.

Acknowledgements

The publication was written at Virtual Vehicle Research GmbH within the scope of the EU project ArchitectECA2030. This project has received funding from the ECSEL Joint Undertaking (JU) under grant agreement No 877539. The JU receives support from the European Union's Horizon 2020 research and innovation program and Germany, Austria, Czech Republic, Netherlands, Lithuania, Latvia, France, Sweden, and Norway. In Austria, the project was also funded by the program "IKT der Zukunft" of the Austrian Federal Ministry for Climate Action (BMK). The work was also jointly supported by the project EUREKA TestEPS funded by the Austrian Research Promotion Agency (FFG) under project No. FO999886466. The authors would like to further acknowledge the financial support within the COMET K2 Competence Centers for Excellent Technologies from the Austrian Federal Ministry for Climate Action (BMK), the Austrian Federal Ministry for Labour and Economy (BMAW), the Province of Styria (Dept. 12) and the Styrian Business Promotion Agency (SFG). The Austrian Research Promotion Agency (FFG) has been authorized for program management. The authors would like to thank the Budapest University of Technology and Economics, Joanneum Research, the Graz University of Technology, Knorr Bremse Hungary, and AVL Hungary for their participation in the M86 measurement campaign and also their consent to make this data publicly available.

Nomenclature

ACC Adaptive Cruise Control

$AD(S)$ Automated Driving (System)

$ADAS$ Advanced Driver Assistance Systems

ADD Automated Driving Demonstrator

AI Artificial Intelligence

$ALKS$ Automated Lane Keeping System

CAN Controller Area Network

DDT Dynamic Driving Task

$DGPS$ Differential GPS

EPS Environment Perception System

$FAIR$ Findable, Accessible, Interoperable, and Reusable

FoV Field of View

$GNSS$ Global Navigation Satellite System

GPS Global Positioning System

$GTAD$ Ground Truth for Automated Driving

ISO International Organization for Standardization

$Lidar$ Light detection and ranging

$NTRIP$ Networked Transport of RTCM via Internet Protocol

ODD Operational Design Domain

ROS Robot Operating System

RTK Real Time Kinematic

SAE Society of Automotive Engineers

TCP/IP Tranmission Control Protocol / Internet Protocol

$UNECE$ UN Economic Commission for Europe

ViF Virtuelles Fahrzeug (Virtual Vehicle Research GmbH)

VRU Vulnerable Road User

References

Agarwal S, Vora A, Pandey G, Williams W, Kourous H and McBride J (2020) Ford multi-av seasonal dataset. *The International Journal of Robotics Research* 39(12): 1367–1376.

Bijelic M, Gruber T, Mannan F, Kraus F, Ritter W, Dietmayer K and Heide F (2020) Seeing through fog without seeing fog: Deep multimodal sensor fusion in unseen adverse weather. In: *Proceedings of the IEEE/CVF Conference on Computer Vision and Pattern Recognition*. pp. 11682–11692.

Blanco-Claraco JL, Moreno-Duenas FA and González-Jiménez J (2014) The málaga urban dataset: High-rate stereo and lidar in a realistic urban scenario. *The International Journal of Robotics Research* 33(2): 207–214.

BME (2020) URL https://www.automateddrive.bme.hu/downloads. Accessed: 2021-11-30.

Caesar H, Bankiti V, Lang AH, Vora S, Liong VE, Xu Q, Krishnan A, Pan Y, Baldan G and Beijbom O (2020) nuscenes: A multimodal dataset for autonomous driving. In: *Proceedings of the IEEE/CVF conference on computer vision and pattern recognition*. pp. 11621–11631.

Chang MF, Lambert J, Sangkloy P, Singh J, Bak S, Hartnett A, Wang D, Carr P, Lucey S, Ramanan D et al. (2019) Argoverse: 3d tracking and forecasting with rich maps. In: *Proceedings of the IEEE/CVF Conference on Computer Vision and Pattern Recognition*. pp. 8748–8757.

Cordts M, Omran M, Ramos S, Rehfeld T, Enzweiler M, Benenson R, Franke U, Roth S and Schiele B (2016) The cityscapes dataset for semantic urban scene understanding. In: *Proceedings of the IEEE conference on computer vision and pattern recognition*. pp. 3213–3223.

Daimler (2021) Drive pilot. URL https://www.daimler.com/innovation/case/autonomous/drive-pilot.html. Accessed: 2021-11-30.

Doll G, Ebel E, Heineke K, Kellner M and Charlotte W (2020) Private autonomous vehicles: The other side of the robo-taxi story. Technical report, McKinsey's Center for Future Mobility and Automotive and Assembly practice. URL https://www.mckinsey.com/industries/automotive-and-assembly/our-insights/. Accessed: 2021-11-26.

Dueser T, Gutenkunst C, Zhao Q, Zhou B, Hary M, Simkin B, Reid A, Woon M, Stachewicz A, Tintinalli J, Cheng C, Graefe G and Tuttas S (2019) A comprehensive approach for the validation of virtual testing toolchains. White paper, IAMTS. URL https://iamts.sae-itc.com/publications. Accessed: 2021-11-30.

Déziel JL, Merriaux P, Tremblay F, Lessard D, Plourde D, Stanguennec J, Goulet P and Olivier P (2021) Pixset : An opportunity for 3d computer vision to go beyond point clouds with a full-waveform lidar dataset.

Ettinger S, Cheng S, Caine B, Liu C, Zhao H, Pradhan S, Chai Y, Sapp B, Qi C, Zhou Y et al. (2021) Large scale interactive motion forecasting for autonomous driving: The waymo open motion dataset. arXiv preprint arXiv:2104.10133.

European Commission (2019) Eu road safety policy framework 2021-2030 - next steps towards "vision zero". URL https://ec.europa.eu/transport/road_safety/what-we-do_en. [Online; accessed 26-November-2021].

Fagnant DJ and Kockelman K (2015) Preparing a nation for autonomous vehicles: opportunities, barriers and policy recommendations. *Transportation Research Part A: Policy and Practice* 77: 167–181. DOI:https://doi.org/10.1016/j.tra.2015.04.003. URL https://www.sciencedirect.com/science/article/pii/S0965856415000804.

Geiger A, Lenz P, Stiller C and Urtasun R (2013) Vision meets robotics: The kitti dataset. *The International Journal of Robotics Research* 32(11): 1231–1237.

Genser S, Muckenhuber S, Solmaz S and Reckenzaun J (2021) Development and experimental validation of an intelligent camera model for automated driving. *Sensors* 21(22). DOI: 10.3390/s21227583. URL https://www.mdpi.com/1424-8220/21/22/7583.

Geyer J, Kassahun Y, Mahmudi M, Ricou X, Durgesh R, Chung AS, Hauswald L, Pham VH, Mühlegg M, Dorn S et al. (2020) A2d2: Audi autonomous driving dataset. arXiv:2004.06320.

Haas S, Solmaz S, Reckenzaun J and Genser S (2023) ViF-GTAD: A new Automotive Data Set with Ground Truth for ADAS/AD Development, Testing and Validation. DOI:10.5281/zenodo.7808255. URL https://doi.org/10.5281/zenodo.7808255.

Hannawald L and Kühn M (2015) Handbuch fahrerassistenzsysteme. In: Winner H, Hakuli S, Lotz F and Singer C (eds.) *H. Winner and S. Hakuli and F. Lotz and C. Singer*, ATZ/MTZ-Fachbuch. Wiesbaden: Springer Fachmedien, pp. 55–70.

Honda (2020) Sensing elite. URL https://global.honda/innovation/technology/automobile/safety/sensing_elite.html. Accessed: 2021-11-30.

Houston J, Zuidhof G, Bergamini L, Ye Y, Chen L, Jain A, Omari S, Iglovikov V and Ondruska P (2020) One thousand and one hours: Self-driving motion prediction dataset. arXiv preprint arXiv:2006.14480.

Huang X, Wang P, Cheng X, Zhou D, Geng Q and Yang R (2020) The apolloscape open dataset for autonomous driving and its application. *IEEE Transactions on Pattern Analysis and Machine Intelligence* 42(10): 2702–2719. DOI:10.1109/tpami.2019.2926463. URL http://dx.doi.org/10.1109/TPAMI.2019.2926463.

ISO 20035:2019(E) (2019) Intelligent transport systems — cooperative adaptive cruise control systems (cacc) — performance requirements and test procedures. Standard, International Organization for Standardization (ISO). URL https://www.iso.org/standard/66879.html.

ISO PAS 1883:2020 (2020) Operational design domain (odd) taxonomy for an automated driving system (ads). specification. Standard, British Standards Institution (BSI). URL https://www.bsigroup.com/en-GB/CAV/pas-1883/.

Kalra N and Paddock SM (2016) How many miles of driving would it take to demonstrate autonomous vehicle reliability? Technical report, RAND Corporation. URL https://www.rand.org/pubs/research_reports/RR1478.html. Accessed: 2022-02-25.

Ligocki A, Jelinek A and Zalud L (2020) Brno urban dataset-the new data for self-driving agents and mapping tasks. In: *2020 IEEE International Conference on Robotics and Automation (ICRA)*. IEEE, pp. 3284–3290.

Lundgren J and Tapani A (2006) Evaluation of safety effects of driver assistance systems through traffic simulation. *Transportation Research Record* 1953(1): 81–88. DOI:10.1177/0361198106195300110.

Maddern W, Pascoe G, Linegar C and Newman P (2017) 1 year, 1000 km: The oxford robotcar dataset. *The International Journal of Robotics Research* 36(1): 3–15.

Patil A, Malla S, Gang H and Chen YT (2019) The h3d dataset for full-surround 3d multi-object detection and tracking in crowded urban scenes. arXiv:1903.01568.

Pitropov M, Garcia DE, Rebello J, Smart M, Wang C, Czarnecki K and Waslander S (2020) Canadian adverse driving conditions dataset. *The International Journal of Robotics Research* 40(4-5): 681–690. DOI:10.1177/0278364920979368. URL http://dx.doi.org/10.1177/0278364920979368.

Rainer Aue JB Pierre RMai (2022) Sensor model classification. URL https://gitlab.setlevel.de/open/processes_and_traceability/credible_simulation_process_framework/-/blob/main/SETLevel_sensor_models_classification.pdf.

Reckenzaun J, Csanady L, Eichberger A, Engelstein A, Hörmann L, Kiss T, Luley P, Rüther M, Schwarz S, Strasser-Krauss T, Solmaz S, Soos G, Tihanyi V, Turoczi A, Weissensteiner P and Zhou J (2022) Transnational testing, operation and certification of automated driving systems: Perspective from testeps and central system eureka projects. In: *2022 International Conference on Connected Vehicle and Expo (ICCVE)*. pp. 1–6. DOI:10.1109/ICCVE52871.2022.9742896.

SAE J3016 (2021) Taxonomy and definitions for terms related to driving automation systems for on-road motor vehicles. Standard, SAE On-Road Automated Driving (ORAD) committee, Geneva, CH. URL https://saemobilus.sae.org/content/J3016_202104/.

Scale (2021) Pandaset data set. http://pandaset.org/. [Online; accessed 22-October-2021].

SetLevel Project (2022) Simulation-based engineering and testing of automated driving. URL https://setlevel.de/en. Accessed: 2023-04-24.

Sheeny M, De Pellegrin E, Mukherjee S, Ahrabian A, Wang S and Wallace A (2020) Radiate: A radar dataset for automotive perception. *arXiv preprint arXiv:2010.09076* 3(4): 7.

Solmaz S, Holzinger F, Mischinger M, Rudigier M and Reckenzaun J (2021a) Novel hybrid-testing paradigms for automated vehicle and adas function development. In: Zakir Abdul Hamid U and Al-Turjman F (eds.) *Towards Connected and Autonomous Vehicle Highways*. Springer, Cham.: EAI/Springer Innovations in Communication and Computing, pp. 193–228.

Solmaz S, Rudigier M, Mischinger M and Reckenzaun J (2021b) Hybrid testing: A vehicle-in-the-loop testing method for the development of automated driving functions. *SAE International Journal of Connected and Automated Vehicles* 4(1): 133–148. DOI:https://doi.org/10.4271/12-04-01-0011. URL https://doi.org/10.4271/12-04-01-0011.

Tihanyi V, Tettamanti T, Csonthó M, Eichberger A, Ficzere D, Gangel K, Hörmann LB, Klaffenböck MA, Knauder C, Luley P, Magosi ZF, Magyar G, Németh H, Reckenzaun J, Remeli V, Rövid A, Ruether M, Solmaz S, Somogyi Z, Soós G, Szántay D, Tomaschek TA, Varga P, Vincze Z, Wellershaus C and Szalay Z (2021) Motorway measurement campaign to support r&d activities in the field of automated driving technologies. *Sensors* 21(6). DOI:10.3390/s21062169. URL https://www.mdpi.com/1424-8220/21/6/2169.

UNECE R157 (2021) Uniform provisions concerning the approval of vehicles with regard to automated lane keeping systems (alks). https://unece.org/transport/documents/2021/03/standards/un-regulation-no-157-automated-lane-keeping-systems-alks. Accessed: 2021-11-30.

UNECE WP.29 (2022) New assessment/test method for automated driving (natm) master document (final draft). URL https://unece.org/sites/default/files/2022-05/WP.29-187-08e.pdf.

Wilson B, Qi W, Agarwal T, Lambert J, Singh J, Khandelwal S, Pan B, Kumar R, Hartnett A, Pontes JK, Ramanan D, Carr P and Hays J (2021) Argoverse 2: Next generation datasets for self-driving perception and forecasting. In: *Proceedings of the Neural Information Processing Systems Track on Datasets and Benchmarks (NeurIPS Datasets and Benchmarks 2021)*.

Yan Z, Sun L, Krajnik T and Ruichek Y (2020) Eu long-term dataset with multiple sensors for autonomous driving. arXiv:1909.03330.

Yu F, Chen H, Wang X, Xian W, Chen Y, Liu F, Madhavan V and Darrell T (2020) Bdd100k: A diverse driving dataset for heterogeneous multitask learning. arXiv:1805.04687.